

3. BACKGROUND AND REGIONAL SETTING¹

Brian Taylor²

THEMATIC INTRODUCTION

The processes by which continental lithosphere accommodates strain during rifting and the initiation of seafloor spreading are presently known primarily from the study of either (1) passive margins bordering rifted continents where extensional tectonics have long ceased and evidence for active tectonic processes must be reconstructed from a record that is deeply buried in post-rift sediments and thermally equilibrated or (2) regions of intracontinental extension, such as East Africa, the U.S. Basin and Range, and the Aegean, where extension has occurred recently by comparison to most passive margin examples, but has not proceeded to the point of continental breakup.

One particularly controversial conjecture from these studies is that the larger normal detachment faults dip at low angles and accommodate very large amounts of strain through simple shear of the entire lithosphere. The role of low-angle normal detachment faults has been contested strongly, both on observational and theoretical grounds. It has been suggested that intracontinental detachments have been misinterpreted and actually formed by rollover of originally high-angle features, or that they occur at the brittle/ductile boundary in a pure shear system. Theoretically, it has been shown that normal faulting on detachment surfaces would require that the fault be extremely weak—almost frictionless—to allow horizontal stresses to cause failure on low-angle planes. The growing evidence for a weak fault and strong crust associated with motion on the San Andreas transform fault supports the weak normal detachment fault model, and models in which low-angle detachment faulting is an essential mechanism of large-scale strain accommodation abound in the literature.

Nevertheless, the mechanisms by which friction might be effectively reduced on low-angle normal fault surfaces are not understood. One possibility is that active shearing in the fault zone creates a strong per-

¹Examples of how to reference the whole or part of this volume.

²School of Ocean and Earth Science and Technology, University of Hawaii at Manoa, 2525 Correa Road, Honolulu, HI 96822-2285, U.S.A. taylor@soest.hawaii.edu

meability contrast with the surrounding crust (by opening cracks more quickly than precipitation can heal them), allowing pore-pressure distributions that are high and near to the fault-normal compressive stress within the fault zone, but decrease with distance into the adjacent crust (Rice, 1992; Axen, 1992). Others have suggested that fluid-rock reactions form phyllosilicates in the fault zone that are particularly weak because of their well-developed fabrics (Wintsch et al., 1995). Alternatively, principal-stress orientations may be rotated into configurations consistent with low-angle faulting, although it has not been demonstrated that the magnitudes of reoriented stresses are sufficient to initiate and promote such slip (Wills and Buck, 1997). Testing for such fault-proximal high permeability and pore pressures, for the presence of weak phyllosilicates, and/or for local rotation of stress axes, requires drilling into an active system. This would also allow determination of the properties of the fault rock at depth (do they exhibit reduced frictional strength at higher slip velocities, consistent with unstable sliding and observed earthquakes?), as well as studies of the mechanisms by which fluid-rock reactions affect deformation (constitutive response, frictional stability, long-term fault strength; see Hickman et al., 1993, and Barton et al., 1995, for extensive discussion of the mechanical involvement of fluids in faulting, and Wernicke, 1995, for a review of low-angle normal faulting).

A primary objective of Leg 180 was to drill into and characterize an active low-angle normal fault—the extreme example of the low-stress fault paradox. Such a fault, dipping 25°–30°, has been imaged north of Moresby Seamount where seafloor spreading in the western Woodlark Basin is breaking into the continental lithosphere of Papua New Guinea (see Fig. F1; also “Introduction,” p. 1, in the “Leg 180 Summary” chapter).

The western Woodlark Basin is arguably the best characterized region of active continental breakup. The proximity of a seismogenic low-angle normal fault that has been imaged by seismic reflection data and zero-offset conjugate margins that are about to be penetrated by seafloor spreading is unique. This region affords the possibility to definitively tie together the sedimentology, magmatism, and structures of (incipient) conjugate margins before they are separated and buried by a subsequent history of seafloor spreading and sedimentation. Determining these parameters was a second objective of Leg 180 with the intent to use them as local ground truth to be input into regional models for the timing and amount of extension prior to spreading initiation. A precruise description of the region is provided below.

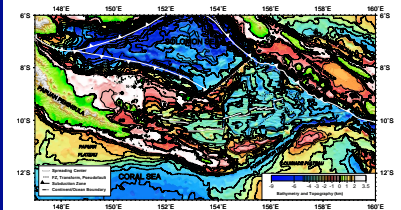
REGIONAL SETTING

Research Programs in the Woodlark Basin and Papuan Peninsula

Several research programs in the last decade have significantly improved our understanding of the regional geological and geophysical setting of rifting into the Papuan Peninsula:

1. Sidescan and underway geophysical surveys have provided bathymetry, acoustic imagery, magnetization, and gravity maps, and allowed detailed reconstructions of the spreading history (Taylor et al., 1995, 1996, in press; Goodliffe et al., 1997; “Geo-

F1. Physiographic features and plate boundaries of the Woodlark Basin region, p. 13.



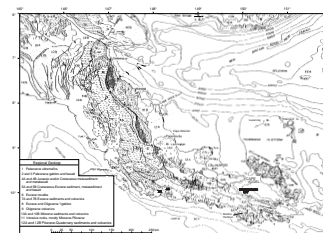
- physical Data and Processing,”** p. 2, in the “Data Report: Marine Geophysical Surveys of the Woodlark Basin Region” chapter; Goodliffe, 1998).
2. Multichannel seismic reflection surveys reveal the upper crustal architecture of the rifting region, including the presence of low-angle normal faults (see Fig. F4, p. 35, in the “Leg 180 Summary” chapter; Mutter et al., 1996; Taylor et al., 1996, in press; Abers et al., 1997; **“Morphology and Seismicity,”** p. 4, in the “Data Report: Marine Geophysical Surveys of the Woodlark Basin Region” chapter).
 3. The PACLARK and SUPACLARK series of cruises in 1986–1991 (Binns et al., 1987, 1989, 1990; Lisitsin et al., 1991; Benes et al., 1994) included dredging, coring, camera and video observations, and seven *Mir* submersible dives. The bottom samples include Normal Mid-Ocean Ridge Basalt (N-MORB) from the youngest spreading segments, as well as greenschist facies metamorphics from the lower north flank of Moresby Seamount. In contrast, a 1995 site survey dredged late Pliocene (synrift) sedimentary rocks from the upper south flank of Moresby Seamount (Taylor et al., 1996). Their presence is not compatible with exhumation of lower crust in the Pliocene–Pleistocene to form Moresby Seamount as a synrift metamorphic core complex.
 4. Abers (1991) and Abers et al. (1997) determined source parameters and relocated earthquakes in the rifting region. The focal mechanisms are all extensional or strike slip with northerly tension axes (see Fig. F2, p. 33, in the “Leg 180 Summary” chapter). Several are consistent with slip on shallow-dipping normal faults.
 5. Studies of metamorphic core complexes on the Papuan Peninsula and D’Entrecasteaux and Misima Islands show that (a) they are associated with Pliocene–Pleistocene granodiorite intrusions and amphibolite-facies ductile shear zones; (b) some have been rapidly exhumed from ~30 km depth (7–11 kilobar [kb]) in the last 4 m.y., whereas others were uplifted to near the surface by the early Miocene; (c) uplift continues (forming topography up to 2.5 km); and (d) they are very three dimensional and regionally discontinuous (or varying in grade) along strike (Davies and Warren, 1988, 1992; Hill, 1987, 1990, 1994, 1995; Hill et al., 1992, 1995; Hill and Baldwin, 1993; Baldwin et al., 1993; Lister and Baldwin, 1993; Baldwin and Ireland, 1995).
 6. The Papuan Ultramafic Belt is a late Paleocene to early Eocene suprasubduction zone ophiolite with gabbros and boninites $^{40}\text{Ar}/^{39}\text{Ar}$ dated at 59 Ma (R. Duncan, pers. comm., 1993; Walker and McDougall, 1982), P4 (late Paleocene) foraminifer-bearing micrites overlying the basalts, with tonalite-diorite-dacite intrusions K/Ar dated at 57–47 Ma (Rogerson et al., 1993). This revision to dating of the Papuan Peninsula basement (Fig. F2) allows a simplified geological evolution for the region, as outlined below.

Papuan Crustal Evolution

Paleogene Subduction and Collision

Much of the Papuan Peninsula is 1–3 km above sea level and is underlain by a crust 25–50 km thick (Finlayson et al., 1976). Major oro-

F2. Regional geology of eastern Papua, p. 14.



genic thickening of the crust occurred following the northeast subduction and partial accretion of a thick sequence of dominantly Cretaceous to Eocene strata beneath a late Paleocene–early Eocene island arc that includes the Papuan Ultramafic Belt (PUB), Milne Basic Complex, and Cape Vogel boninites (Davies and Jaques, 1984; Davies et al., 1984; Rogerson et al., 1987, 1993). Collision of the Australian (Papuan) continental margin plateau caused subduction to cease and uplifted the accretionary complex (Owen Stanley Metamorphics) by the early Miocene (Rogerson et al., 1987). Metabasites in the Emo metamorphics and Suckling-Dayman massif (the latter with a cover of Maastrichtian micrites) have been exhumed from 7 to 12 kb (25–35 km) and may represent slivers of the subducted Cretaceous oceanic crust (Unit 4B in Fig. F2; Davies, 1980; Worthing, 1988).

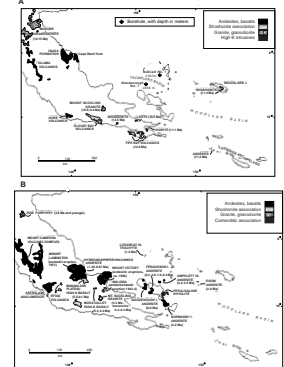
The pre-Miocene geology of the islands on the Pocklington and Woodlark Rises is similar to that of the Papuan Peninsula, with Owen Stanley Metamorphics in the south (Misima, Tagula, and Rossel Islands; Fig. F1) and Milne Basic Complex outcrops on Woodlark Island (Davies and Smith, 1971; Ashley and Flood, 1981). Likewise, upper Paleocene volcanics are present at the base of the Nubiam-1 well (Stewart et al., 1986; Fig. F1), west of the Trobriand Islands. The metamorphic core complexes on the D'Entrecasteaux Islands have a core of Owen Stanley Metamorphics and a cover of metamorphosed ultramafics, unmetamorphosed gabbros, and lower Miocene and younger volcanogenic sediments and limestone (Davies and Warren, 1988; Fig. F2).

Miocene–Quaternary Arc and Forearc

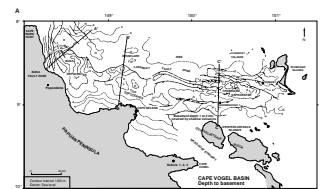
Superimposed on this Paleogene basement is widespread middle Miocene–Holocene arc magmatism (Fig. F3; Smith and Milsom, 1984) associated with southwest subduction of the Solomon Sea Basin at the Trobriand Trough. The main volcanic arc is calc-alkaline, whereas minor volcanism on the outer forearc high (Lusancay and Woodlark Islands) is high-K (shoshonitic). Historical arc volcanism and a deforming accretionary prism are compatible with present-day slow subduction at the Trobriand Trough (Hamilton, 1979; Davies and Jaques, 1984; Cooper and Taylor, 1987; Lock et al., 1987; Pegler et al., 1995), although this remains controversial given the small number of intermediate-depth earthquakes beneath the region (Abers and Roecker, 1991) and the lack of ¹⁰Be in the lavas of Mount Lamington (Gill et al., 1993). The geochemistry of the volcanics reveals melting and mixing of at least three magma sources: (1) subduction-modified mantle supplied the calc-alkaline arc volcanism; (2) this mantle, with the addition of partial melts from upwelling aesthenosphere, produced the comenditic (transitional basalt-peralkaline rhyolites) series around Dawson Strait (between Fergusson and Normanby Islands); and (3) contamination by lower crust of Australian affinity formed minor high-K trachytes (see Smith, 1976; Hegner and Smith, 1992; Stolz et al., 1993; and references therein).

The Cape Vogel Basin (Fig. F4) is the western part of the Neogene Trobriand forearc basin that parallels the Trobriand Trough to the south of an outer forearc high (with an associated 150–200 mGal free-air gravity anomaly) topped by the Lusancay-Trobriand-Woodlark Islands (Figs. F1, F2, F4). The stratigraphy is known from onshore exposures and the Kukuia wells on the Cape Vogel Peninsula, and especially from the offshore wells (Goodenough-1 and Nubiam-1; Figs. F1, F4, F5) drilled by Amoco and partners in 1973 following 2 yr of regional basin studies,

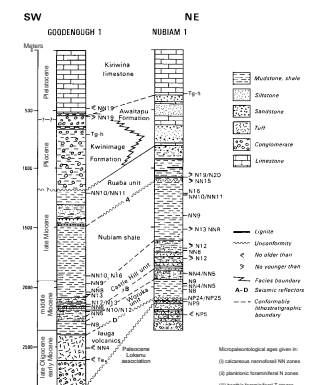
F3. Miocene and Pliocene–Pleistocene volcanism in eastern Papua, p. 15.



F4. Cape Vogel Basin depth to basement and cross sections, p. 16.



F5. Goodenough-1 and Nubiam-1 wells lithologies and biostratigraphy, p. 18.



including the collection of 2250 km of seismic reflection data (Figs. F6, F7; Tjhin, 1976; Pinchin and Bembrick, 1985; Stewart et al., 1986; and Francis et al., 1987). It is characterized by early(?)–middle Miocene subsidence, volcanism, and deep-marine sedimentation; late Miocene uplift and erosion (1–2 km) of the margins; and Pliocene coarse clastic (from uplift of the Papuan Peninsula and D’Entrecasteaux Islands to the south) and Quaternary carbonate, shallow-water sedimentation during broad subsidence (Tjhin, 1976; Stewart et al., 1986; Francis et al., 1987; Davies and Warren, 1988).

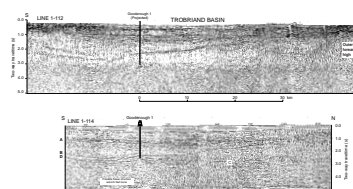
The basin experienced late Miocene inversion in the northwest, but its center continues to subside in the southeast (Figs. F4, F5, F6; Pinchin and Bembrick, 1985). Several key unconformities are regionally correlatable on reflection seismic lines within the basin and were penetrated by the exploration wells. Of particular importance to Leg 180 results is unconformity A and the overlying Ruaba unit. The Ruaba unit is a distinctive facies characterized by sandstones, shales, and claystones with occasional lignite and conglomerate, and it is interpreted to have been deposited in a paralic environment, including nonmarine deltas to mid-neritic prodeltas (Stewart et al., 1986; Francis et al., 1987). The top of the unit is dated as NN10/NN11 at Goodenough-1, and there, as well as at Nubiam-1, the unit is younger than the underlying Nubiam shale whose upper section belongs to biozones NN10 and N16 (Fig. F5). Thus, the regional unconformity A is definitely younger than 9.63 Ma (the base of Zone NN10) and possibly younger than 8.6 Ma (the top of Zone NN10) (Berggren et al., 1995). That the forearc basin filled to near sea level in the late Miocene is inferred from the seismic sequences that prograde northward across the basin beneath unconformity A to a depocenter just south of the outer forearc high (e.g., Fig. F7).

The Trobriand Trough, the outer forearc structural and gravity high, and the Trobriand forearc basin terminate near Woodlark Island. Farther east, the Woodlark and Pocklington Rises were not a Pliocene–Pleistocene arc-forearc system. Rather, the northern edge of the eastern Woodlark Rise was a transform margin. Seismicity and sidescan data indicate that it is still an active right-lateral fault (Fig. F1). Thus, the Woodlark Basin east of 153.5°E did not originate as a backarc basin in that the eastern Woodlark and Pocklington Rises were not active island arcs (Weissel et al., 1982). Nevertheless, the locus of present rifting (see “Pliocene–Pleistocene Rifting,” p. 5) does, and did since the latest Miocene bisect an active continental volcanic arc with inherited crustal asymmetry, having a Neogene forearc basin to the north and a Paleogene accretionary/collision complex to the south.

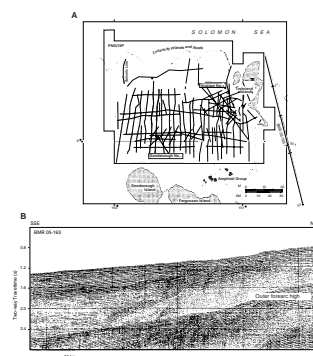
Pliocene–Pleistocene Rifting

Shallow seismicity, with extensional and strike-slip focal mechanisms having northerly tension axes, is concentrated between Ferguson and Woodlark Islands and extends westward into the Papuan Peninsula at 9°S–10°S to about 148°E (see Fig. F2, p. 33, in the “Leg 180 Summary” chapter; Weissel et al., 1982; Abers, 1991; Abers et al., 1997). Pliocene–Pleistocene extension has produced three flooded grabens (Mullins Harbour, Milne Bay, and Goodenough Bay) on the eastern extremity of the Papuan Peninsula with associated rift-flank subaerial uplift to over 500 m (Smith and Simpson, 1972). Metamorphic core complexes on the D’Entrecasteaux Islands and in the Suckling-Dayman massif on the Papuan Peninsula were also exhumed during the Pliocene–Pleistocene (Davies, 1980; Davies and Warren, 1988; Hill, 1990). The best structural studies, geothermometry, geobarometry, and

F6. Trobriand Basin seismic reflection profiles, p. 19.



F7. Trobriand Basin track lines and sparker profile BMR 05-163, p. 20.



age dating of these complexes have been conducted on Goodenough and Fergusson Islands (Davies and Warren, 1992; Hill et al., 1992, 1995; Hill and Baldwin, 1993; Baldwin et al., 1993; Lister and Baldwin, 1993; Hill, 1994; Baldwin and Ireland, 1995). There, normal movement along a 0.3- to 1.5-km-thick ductile mylonitic shear zone resulted in the uplift of deep metamorphic rocks and the juxtaposition of unmetamorphosed cover rocks. Granodioritic intrusion then focused uplift on several domes, offset by strike-slip faults. The ductile shear zones were brecciated and truncated by brittle faults late in their history. These dome structures are juxtaposed along strike with regions of significantly less unroofing, such as the low-grade (greenschist) eastern halves of both Normanby and Misima islands.

Woodlark Basin Evolution

The Woodlark Basin has been opening since 6 Ma (Chron 3An.1n), at which time the westernmost spreading segment was located east of 157°E (Taylor, 1987; Taylor and Exon, 1987; Goodliffe, 1998; Taylor et al., 1999). The pole of early opening was at 9.3°S, 147°E, with a rotation rate of 4.234°/m.y., and the spreading center migrated westward through time (Goodliffe, 1998; Taylor et al., 1999). The spreading center grew discontinuously, stepping across Simbo Transform (156.5°E) at ~3.6 Ma and Moresby Transform (154.2°E) at ~2 Ma, to reach 151.8°E by 0.7 Ma. The 500-km-long spreading axis reoriented synchronously ~80 ka, producing the present discordance of the spreading axes with the Brunhes Chron boundary, following a change in the pole of opening (recorded by the fracture zones) at 0.52 Ma to 12°S, 144°E, 2.437°/m.y. (Goodliffe et al., 1997; Goodliffe, 1998; Taylor et al., 1999). This pole is located within the error ellipse of the position of the current Australia-Woodlark Euler pole (10.8°S, 145.2°E, 1.86°/m.y.) determined geodetically by Tregoning et al. (1998) but predicts opening rates ~30% faster over the last 0.52 m.y. than at present.

The sidescan and geophysical data show that the rifting-to-spreading transition involves both nucleation of discrete spreading cells and organized ridge propagation (Taylor et al., 1995). Two ridge propagation events into the margin at 153°E formed continental slivers surrounded by oceanic crust (Fig. F1). Spreading is about to propagate into this margin again. Rifting of the conjugate margins continues for ~1 m.y. after spreading has separated them. Extension does not immediately localize to the ridge axis, as shown by the present overlap between spreading and seismogenic margin faulting, and by inwardly curved seafloor fabric and magnetic anomalies that require nonrigid margin reconstructions. The continental breakup proceeds by successive phases of rifting localization, spreading center nucleation, spreading center propagation (sometimes stalling), and then a jump across an offset to the next site of localized rifting (Taylor et al., 1999). As a result of spreading propagation and, most recently, synchronous reorientation, there is no simple relation between seafloor spreading segmentation and margin rift segmentation. The major spreading center offsets all began as overlapping and/or propagating nontransform offsets and many continue in that mode. The Moresby and 155°10'E transforms initiated by crosscutting previous rift structures to link spreading segments that had nucleated in, and/or propagated into, offset continental rifts (Taylor et al., 1999). They did not evolve from transfer/transform faults or aulocogens in the rifted margins. There is no evidence for thermal uplift or igneous underplating of the Moresby Transform continental margins as spread-

ing axes pass by them, including where spreading segments abut the transform continent/ocean boundary segments today.

Seismic reflection data indicate a very sharp (<5 km wide at the surface) transition from rifted crust to oceanic crust (Taylor et al., 1999). There are no dipping reflector sequences indicative of excessive lava production and high degrees of mantle partial melting, but there are small volcanoes a few kilometers in diameter that often erupt along margin faults. Indeed, the initial seafloor spreading lavas indicate low degrees of partial melting: basalts from the youngest spreading segment, just east of Moresby Seamount, have $Na_8 = 3.1$ (Binns and Whitford, 1987; Danyushevsky et al., 1993; Dril, 1997). Other young axial lavas include Fe-Ti basalts, and low- and high-Si andesites with evidence for both mantle heterogeneity and crustal contamination.

Drilling Area

The rifting region just ahead of the apex of spreading has been imaged by several seismic reflection and swath bathymetry surveys (Mutter et al., 1993, 1996; Goodliffe et al., 1993; **“Geophysical Data and Processing,”** p. 2, in the “Data Report: Marine Geophysical Surveys of the Woodlark Basin Region” chapter; Taylor et al., 1996, in press). Continental breakup is focused currently on an asymmetric rift basin bounded on the south by a low-angle ($27^\circ \pm 3^\circ$), curvi-planar, normal detachment that is imaged over the full depth extent of the seismogenic zone (3–9 km; Fig. F4, p. 35, in the “Leg 180 Summary” chapter; Taylor et al., 1999). The detachment forms the north slope of Moresby Seamount. The rift basin has >2 km of sedimentary fill beneath ~3 km of water and is bounded on the north by an antithetic normal fault that dips ~45°S. The margin further north, including a pre-rift (Trobriand forearc) sedimentary basin and basement sequence, is gently flexed down to the south and unconformably overlapped by syn-rift sediments. The seismic stratigraphy can be reasonably jump-correlated to that in the Trobriand Basin and is interpreted to be a Pliocene–Pleistocene synrift sequence lying unconformably above a Miocene forearc basin sequence on Paleogene volcanic (and metamorphic?) basement (see Figs. F3, p. 34; F5, p. 36; both in the “Leg 180 Summary” chapter). To the south of Moresby Seamount, high-relief rotated fault blocks are commonly overlain by only minor ponded sediments.

Shallow (2–10 km) normal and strike slip faults, with northerly T-axes, bound the north side of the rifting-spreading transition (see Fig. F2, p. 33, in the “Leg 180 Summary” chapter; Abers, 1991; Taylor et al., 1995; Abers et al., 1997). All of the earthquake hypocenters occur within or north of the rift graben, and there are no major extensional structures north of the graben-bounding antithetic fault. Without local seismometers, the teleseismicity has not been definitively associated with the low-angle reflector, but no more likely candidate structure is observed. Furthermore, the seismic stratigraphy cannot be matched without recent faulting on the low-angle reflector.

Two dredges of the northern flank of Moresby Seamount recovered metabasic greenschists, metagabbro, pelitic schist, and minor siliceous phyllite and microgranite (i.e., similar material to the low-grade [greenschist] metamorphics on eastern Normanby and Misima Islands), not the core complex amphibolite metamorphics as on Goodenough, Fergusson, and northwest Normanby (H. Craig, pers. comm., 1986; Binns et al., 1987; J. Hill, pers. comm., 1996). In contrast, a dredge from 541 to 1211 m (~0.7–1.6 s two-way traveltime [TWT]) on the upper south-

ern flank of the Moresby Seamount recovered mainly late Pliocene (Zone N21 = 1.6–3.35 Ma) clastic sedimentary rocks of equivalent facies to the Awaitapu Formation of the Trobriand region in the Cape Vogel Basin (Francis et al., 1987). Benthic foraminifers indicate sediment deposition in water depths of 340–800 m (J. Resig, pers. comm., 1995). These rocks are equivalent to those that we infer lie near the base of the synrift cover sequence in the rift basin and perhaps on the northern margin.

A simplified cross section consistent with the seismic and dredge data available pre-cruise is drawn in Figure F3, p. 34, in the “Leg 180 Summary” chapter, (Taylor et al., 1996). At the end of the Miocene, the Paleogene basement and a forearc basin filled with Miocene sediment were being eroded at or near sea level (Fig. F7). Pliocene rifting formed sediment-filled grabens in the southern orogenically thickened arc province, accompanied by gradual subsidence of the thinner, colder (and therefore stronger) forearc to the north. Stretching during the Quaternary was localized on a low-angle normal fault. The antithetic hanging-wall faults accommodated little additional extension. East of the Trobriand reef front at 151°10'E (Fig. F1) the northern margin flexed down southward and was overlapped by sediments delivered in part via submarine channels incising northward (Fig. F7, p. 39, in the “Leg 180 Summary” chapter). We infer that the reef front formed on the unloaded footwall of a north-south tear fault bounding the down-flexed margin to the west. Recently, continued extension on the low-angle normal fault variably collapsed the hanging-wall graben.

This interpretation predicts ~12 km of heave on the low-angle fault. This compares with 130–145 km of total extension in the 4 m.y. before spreading at this longitude, calculated from the pole of opening derived from seafloor spreading magnetic anomalies (Taylor et al., 1996). If this opening is extrapolated from 4 Ma back to the beginning of spreading at ~6 Ma, then 220 km of total extension is predicted at this longitude (Taylor et al., 1999). Given only minor extension of the northern, flexed margin, we infer that the locus of current extension must be the northernmost of a series of similar structures that extended weak crust to the south, forming the block-faulted Pocklington Rise. The regional estimates predict that this rugged province of mainly inactive faults accommodated ~200 km of total strain as it collapsed from heights comparable to the 3-km-high Owen Stanley Ranges that form the backbone of the Papuan Peninsula. Given that this southern province is only 200 km wide, then, if these regional models are correct, the total strain equals the width of the southern province. Substantial intrusion of arc magmas and/or exhumation of lower crustal material from beneath the northern margin may be required to explain these calculations.

ACKNOWLEDGMENTS

This synthesis benefited from discussions with colleagues working in Papua New Guinea over many years. In particular, I thank Geoff Abers, Ray Binns, Hugh Davies, Geoff Francis, June Hill, Wally Johnson, Rick Rogerson, and many others at the Geological Survey of Papua New Guinea for sharing their work and insights. Support from the U.S. NSF-ODP is greatly appreciated. Reviews by Hugh Davies, Adam Klaus, and Manuel Pubellier helped to improve the manuscript. SOEST contribution #4709.

REFERENCES

- Abers, G.A., 1991. Possible seismogenic shallow-dipping normal faults in the Woodlark-D'Entrecasteaux extensional province, Papua New Guinea. *Geology*, 19:1205–1208.
- Abers, G.A., and Roecker, S.W., 1991. Deep structure of an arc-continent collision: earthquake relocation and inversion for upper mantle *P* and *S* wave velocities beneath Papua New Guinea. *J. Geophys. Res.*, 96:6379–6401.
- Abers, G.A., Mutter, C.Z., and Fang, J., 1997. Shallow dips of normal faults during rapid extension: earthquakes in the Woodlark-D'Entrecasteaux rift system, Papua New Guinea. *J. Geophys. Res.*, 102:15301–15317.
- Ashley, P.M., and Flood, R.H., 1981. Low-K tholeiites and high-K igneous rocks from Woodlark Island, Papua New Guinea. *J. Geol. Soc. Aust.*, 28:227–240.
- Axen, G.J., 1992. Pore pressure, stress increase, and fault weakening in low-angle normal faulting. *J. Geophys. Res.*, 97:8979–8991.
- Baldwin, S.L., and Ireland, T.R., 1995. A tale of two eras: Plio-Pleistocene unroofing of Cenozoic and late Archean zircons from active metamorphic core complexes, Solomon Sea, Papua New Guinea. *Geology*, 23:1023–1026.
- Baldwin, S.L., Lister, G.S., Hill, E.J., Foster, D.A., and McDougall, I., 1993. Thermo-chronologic constraints on the tectonic evolution of active metamorphic core complexes, D'Entrecasteaux Islands, Papua New Guinea. *Tectonics*, 12:611–628.
- Barton, C.A., Zoback, M.D., and Moos, D., 1995. Fluid flow along potentially active faults in crystalline rock. *Geology*, 23:683–686.
- Benes, V., Scott, S.D., and Binns, R.A., 1994. Tectonics of rift propagation into a continental margin: western Woodlark Basin, Papua New Guinea. *J. Geophys. Res.*, 99:4439–4455.
- Berggren, W.A., Kent, D.V., Swisher, C.C., III, and Aubry, M.-P., 1995. A revised Cenozoic geochronology and chronostratigraphy. In Berggren, W.A., Kent, D.V., Aubry, M.-P., and Hardenbol, J. (Eds.), *Geochronology, Time Scales and Global Stratigraphic Correlation*. Spec. Publ.—Soc. Econ. Paleontol. Mineral. (Soc. Sediment. Geol.), 54:129–212.
- Binns, R.A., Scott, S.D., and PACLARK Participants, 1987. Western Woodlark Basin: potential analogue setting for volcanogenic massive sulphide deposits. *Proc. Pac. Rim Congr.*, 87:531–535.
- , 1989. Propagation of sea-floor spreading into continental crust, western Woodlark Basin, Papua New Guinea. *CCOP/SOPAC Misc. Rep.*, 79:14–16.
- Binns, R.A., Scott, S.D., Wheller, G.E., and Benes, V., 1990. Report on the SUPACLARK cruise, Woodlark Basin, Papua New Guinea, April 8–28 1990, RV Akademik Mstislav Keldysh. *CSIRO Rep.* 176R, 1–55.
- Binns, R.A., and Whitford, D.J., 1987. Volcanic rocks from the western Woodlark Basin, Papua New Guinea. *Proc. Pac. Rim Congr.*, 87:525–534.
- Cooper, P., and Taylor, B., 1987. Seismotectonics of New Guinea: a model for arc reversal following arc-continent collision. *Tectonics*, 6:53–67.
- Danyushevsky, L.V., Falloon, T.J., Sobolev, A.V., Crawford, A.J., Carroll, M., and Price, R.C., 1993. The H₂O content of basalt glasses from Southwest Pacific back-arc basins. *Earth Planet. Sci. Lett.*, 117:347–362.
- Davies, H.L., 1980. Folded thrust fault and associated metamorphics in the Suckling-Dayman massif, Papua New Guinea. *Am. J. Sci.*, 280-A:171–191.
- Davies, H.L., and Jaques, A.L., 1984. Emplacement of ophiolite in Papua New Guinea. *Spec. Publ.—Geol. Soc. London*, 13:341–350.
- Davies, H.L., and Smith, I.E., 1971. Geology of eastern Papua. *Geol. Soc. Am. Bull.*, 82:3299–3312.
- Davies, H.L., Symonds, P.A., and Ripper, I.D., 1984. Structure and evolution of the southern Solomon Sea region. *BMR J. Aust. Geol. Geophys.*, 9:49–68.

- Davies, H.L., and Warren, R.G., 1988. Origin of eclogite-bearing, domed, layered metamorphic complexes ("core complexes") in the D'Entrecasteaux islands, Papua New Guinea. *Tectonics*, 7:1–21.
- , 1992. Eclogites of the D'Entrecasteaux Islands. *Contrib. Mineral. Petrol.*, 112:463–474.
- Dril, S.I., Kuzmin, M.I., Tsipukova, S.S., and Zonenshain, L.P., 1997. Geochemistry of basalts from the western Woodlark, Lau and Manus basins: implications for their petrogenesis and source rock compositions. *Mar. Geol.*, 142:57–83.
- Finlayson, D.M., Muirhead, K.J., Webb, J.B., Gibson, G., Furumoto, A.S., Cooke, R.J.S., and Russel, A.J., 1976. Seismic investigation of the Papuan ultramafic belt. *Geophys. J. R. Astron. Soc.*, 29:245–253.
- Francis, G., Lock, J., and Okuda, Y., 1987. Seismic stratigraphy and structure of the area to the southeast of the Trobriand Platform. *Geo-Mar. Lett.*, 7:121–128.
- Gill, J.B., Morris, J.D., and Johnson, R.W., 1993. Time scale for producing the geochemical signature of island arc magmas: U-Th-Po and Be-B systematics in recent Papua New Guinea lavas. *Geochim. Cosmochim. Acta*, 57:4269–4283.
- Goodliffe, A.M., 1998. The rifting of continental and oceanic lithosphere: observations from the Woodlark Basin [Ph.D. thesis]. Univ. Hawaii, Honolulu.
- Goodliffe, A., Taylor, B., Hey, R., and Martinez, F., 1993. Seismic images of continental breakup in the Woodlark Basin, Papua New Guinea. *Eos*, 74:606.
- Goodliffe, A.M., Taylor, B., Martinez, F., Hey, R.N., Maeda, K., and Ohno, K., 1997. Synchronous reorientation of the Woodlark Basin spreading center. *Earth Planet. Sci. Lett.*, 146:233–242.
- Hamilton, W., 1979. Tectonics of the Indonesian region. *Geol. Surv. Prof. Pap. U.S.*, 1078.
- Hegner, E., and Smith, I.E.M., 1992. Isotopic compositions of late Cenozoic volcanics from southeast Papua New Guinea: evidence for multi-component sources in arc and rift environments. *Chem. Geol.*, 97:233–249.
- Hickman, S., Sibson, R., and Bruhn, R. (Eds.), 1993. The mechanical involvement of fluids in faulting. *Open-File Rep.—U.S. Geol. Surv.*, 94–228.
- Hill, E.J., 1987. Active extension in the D'Entrecasteaux Islands, Papua New Guinea. *BMR Res. Symp.*, 87:51–57.
- , 1990. The nature of shear zones formed during extension in eastern Papua New Guinea. *Proc. Pac. Rim Congr.*, 90:537–548.
- , 1994. Geometry and kinematics of shear zones formed during continental extension in eastern Papua New Guinea. *J. Struct. Geol.*, 16:1093–1105.
- , 1995. Extensional deformation of continental crust prior to break-up and sea-floor spreading: a study of Misima Island, Papua New Guinea. *Geol. Soc. Aust.* 9:68–69 (Abstract #40).
- Hill, E.J., and Baldwin, S.L., 1993. Exhumation of high-pressure metamorphic rocks during crustal extension in the D'Entrecasteaux region: Papua New Guinea. *J. Metamorph. Geol.*, 11:261–277.
- Hill, E.J., Baldwin, S.L., and Lister, G.S., 1992. Unroofing of active metamorphic core complexes in the D'Entrecasteaux Islands, Papua New Guinea. *Geology*, 20:907–910.
- , 1995. Magmatism as an essential driving force for formation of active metamorphic core complexes in eastern Papua New Guinea. *J. Geophys. Res.*, 100:10441–10451.
- Lisitzin, A.P., Binns, R.A., Bogdanov, Y.A., Scott, S., Zonenshain, L.P., Gordeyev, V.V., Gurchich, Y.G., Murav'yev, K.G., and Serova, V.V., 1991. Active hydrothermal activity at Franklin Seamount, western Woodlark Sea (Papua New Guinea). *Int. Geol. Rev.*, 33:914–929.
- Lister, G.S., and Baldwin, S.L., 1993. Plutonism and the origin of metamorphic core complexes. *Geology*, 21:607–610.
- Lock, J., Davies, H.L., Tiffin, D.L., Murakami, F., and Kisomoto, K., 1987. The Trobriand subduction system in the western Solomon Sea. *Geo-Mar. Lett.*, 7:129–134.

- Mutter, J.C., Mutter, C.Z., Abers, G., and Fang, J., 1993. Seismic images of low-angle normal faults in the western Woodlark Basin where continental extension yields to seafloor spreading. *Eos*, 74:412.
- Mutter, J.C., Mutter, C.Z., and Fang, J., 1996. Analogies to oceanic behavior in the continental breakup of the western Woodlark Basin. *Nature*, 380:333–336.
- Pegler, G., Das, S., and Woodhouse, J.H., 1995. A seismological study of the eastern New Guinea and the western Solomon Sea regions and its tectonic implications. *Geophys. J. Int.*, 122:961–981.
- Pinchin, J., and Bembrick, C., 1985. Cape Vogel Basin, PNG — tectonics and petroleum potential. In *14th BMR Symposium extended abstracts: petroleum geology of South Pacific island countries*. Bur. Miner. Resour. Aust. Rec., 32:31–37.
- Rice, J.R., 1992. Fault stress states, pore pressure distributions, and the weakness of the San Andreas fault. In Evans, B., and Wong, T.-F. (Eds.), *Fault Mechanics and Transport Properties of Rocks: a Festschrift in Honor of W. F. Brace*: San Diego (Academic Press), 475–503.
- Rogerson, R., Hilyard, D., Francis, G., and Finlayson, E., 1987. The foreland thrust belt of Papua New Guinea. *Proc. Pac. Rim Congr.*, 87:579–583.
- Rogerson, R., Queen, L., and Francis, G., 1993. The Papuan ultramafic belt arc complex. In Wheller, G.E. (Ed.), *Islands and basins: correlation and comparison of onshore and offshore geology*. CCOP/SOPAC Misc. Rept. 159:28–29.
- Smith, I.E., and Simpson, C.J., 1972. Late Cenozoic uplift in the Milne Bay area, eastern Papua New Guinea. *Bull.—Bur. Miner. Resour., Geol. Geophys. (Aust.)*, 125:29–35.
- Smith, I.E.M., 1976. Peralkaline rhyolites from the D'Entrecasteaux Islands, Papua New Guinea. In Johnson, R.W. (Ed.), *Volcanism in Australasia*: Amsterdam (Elsevier), 275–285.
- Smith, I.E.M., and Milsom, J.S., 1984. Late Cenozoic volcanism and extension in eastern Papua. In Kokelaar, B.P., and Howells, M.F. (Eds.), *Marginal basin geology*. Geol. Soc. Spec. Publ. London, 16:163–171.
- Stewart, W.P., Francis, G., and Deibert, D.H., 1986. Hydrocarbon potential of the Cape Vogel Basin, Papua New Guinea. *Geol. Surv. Papua N. G. Rep. No. 86/10*.
- Stolz, A.J., Davies, G.R., Crawford, A.J., and Smith, I.E.M., 1993. Sr, Nd and Pb isotopic compositions of calc-alkaline and peralkaline silicic volcanics from the D'Entrecasteaux Islands, Papua New Guinea, and their tectonic significance. *Mineral. and Petrol.*, 47:103–126.
- Taylor, B., 1987. A geophysical survey of the Woodlark-Solomons region. In Taylor, B., and Exon, N.F. (Eds.), *Marine Geology, Geophysics, and Geochemistry of the Woodlark Basin-Solomon Islands*. Circum-Pac. Council. Energy Mineral Resour., *Earth Sci. Ser.*, 7:25–48.
- Taylor, B., and Exon, N.F., 1987. An investigation of ridge subduction in the Woodlark-Solomons region: introduction and overview. In Taylor, B., and Exon, N.F., *Marine Geology Geophysics, and Geochemistry of the Woodlark Basin-Solomon Islands*. Circum-Pac. Council. Energy Mineral Resour., *Earth Sci. Ser.*, 7:1–24.
- Taylor, B., Goodliffe, A., Martinez, F., and Hey, R., 1995. Continental rifting and initial sea-floor spreading in the Woodlark Basin. *Nature*, 374:534–537.
- Taylor, B., Goodliffe, A.M., and Martinez, F., 1999. How continents break up: insights from Papua New Guinea. *J. Geophys. Res.*, 104:7497–7512.
- Taylor, B., Mutter, C., Goodliffe, A., and Fang, J., 1996. Active continental extension: the Woodlark Basin. *JOI/USSAC Newsl.*, 9:1–4.
- Tjhin, K.T., 1976. Trobriand Basin exploration, Papua New Guinea. *APEA J.*, 16:81–90.
- Tregoning, P., Lambeck, K., Stolz, A., Morgan, P., McClusky, S., van der Beek, P., McQueen, H., Jackson, R., Little, R., Laing, A., and Murphy, B., 1998. Estimation of current plate motions in Papua New Guinea from global positioning system observations. *J. Geophys. Res.*, 103:12181–12203.
- Walker, D.A., and McDougall, I., 1982. $^{40}\text{Ar}/^{39}\text{Ar}$ and K-Ar dating of altered glassy volcanic rocks: the Dabi Volcanics. *Geochim. Cosmochim. Acta*, 46:2181–2190.

- Weissel, J.K., Taylor, B., and Karner, G.D., 1982. The opening of the Woodlark basin, subduction of the Woodlark spreading system, and the evolution of northern Melanesia since mid-Pliocene time. *Tectonophysics*, 87:253–277.
- Wernicke, B., 1995. Low-angle normal faults and seismicity: a review. *J. Geophys. Res.*, 100:20159–20174.
- Wills, S., and Buck, W.R., 1997. Stress-field rotation and rooted detachment faults: a Coulomb failure analysis. *J. Geophys. Res.*, 102:20503–20514.
- Wintsch, R.P., Christoffersen, R., and Kronenberg, A.K., 1995. Fluid-rock reaction weakening of fault zones. *J. Geophys. Res.*, 100:13021–13032.
- Worthing, M.A., 1988. Petrology and tectonic setting of blueschist facies metabasites from the Emo metamorphics of Papua New Guinea. *Aust. J. Earth Sci.*, 35:159–168.

Figure F1. Major physiographic features and active plate boundaries of the Woodlark Basin region. E = Egum Atoll, G = Goodenough Island, GB = Goodenough Basin, F = Fergusson Island, L = Lusancay Islands, M = Misima Island, MB = Milne Bay, MH = Mullins Harbour, MS = Moresby Seamount, MT = Moresby transform fault, N = Normanby Island, R = Rossel Island, ST = Simbo transform fault, T = Tagula Island, TR = Trobriand Islands, W = Woodlark Island. Exploration wells Goodenough-1 and Nubiam-1 are labeled G-1 and N-1.

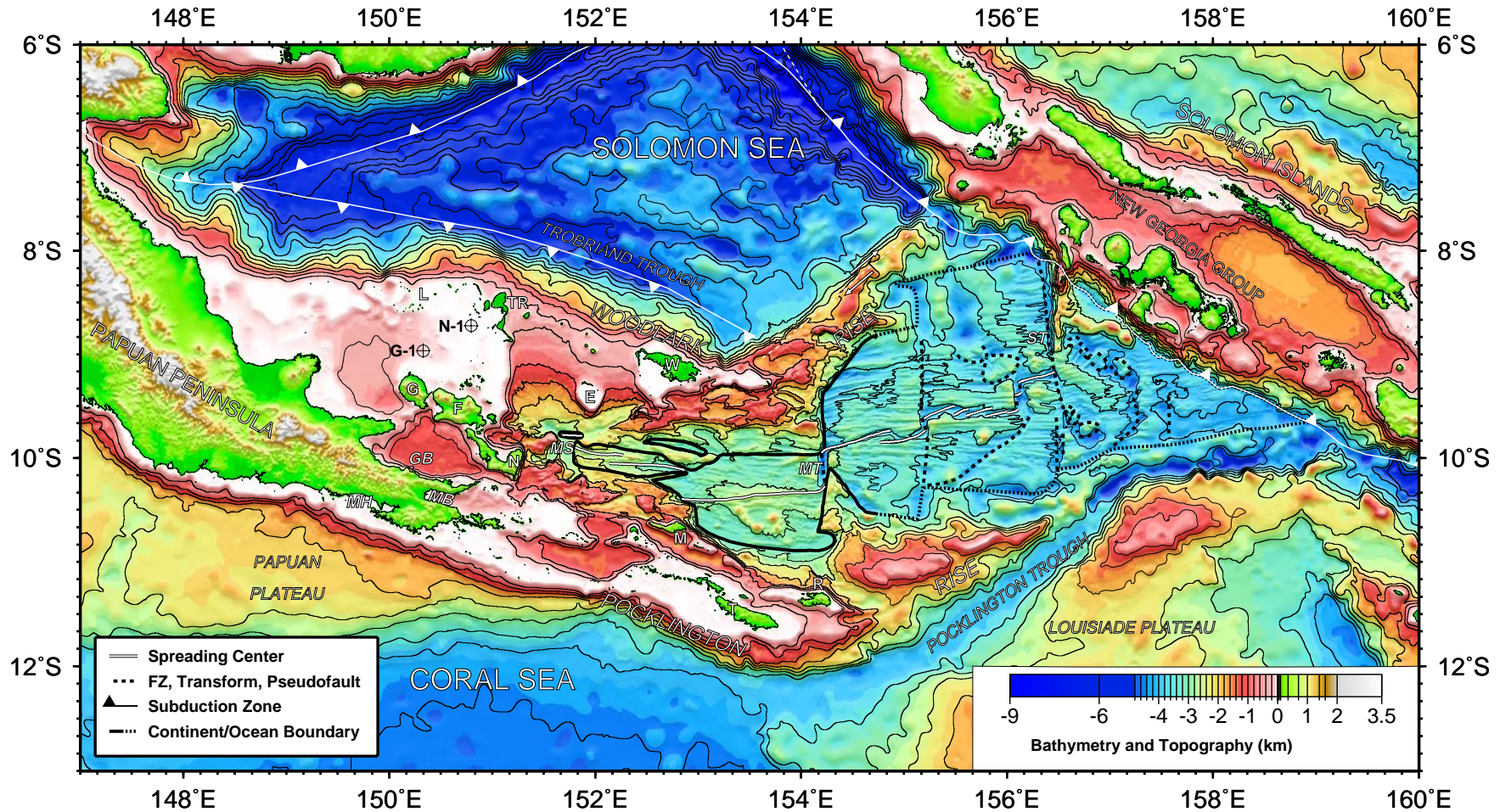


Figure F2. Regional geology of eastern Papua, modified after Davies and Jaques (1984). E = Emo metamorphics, SD = Suckling-Dayman massif.

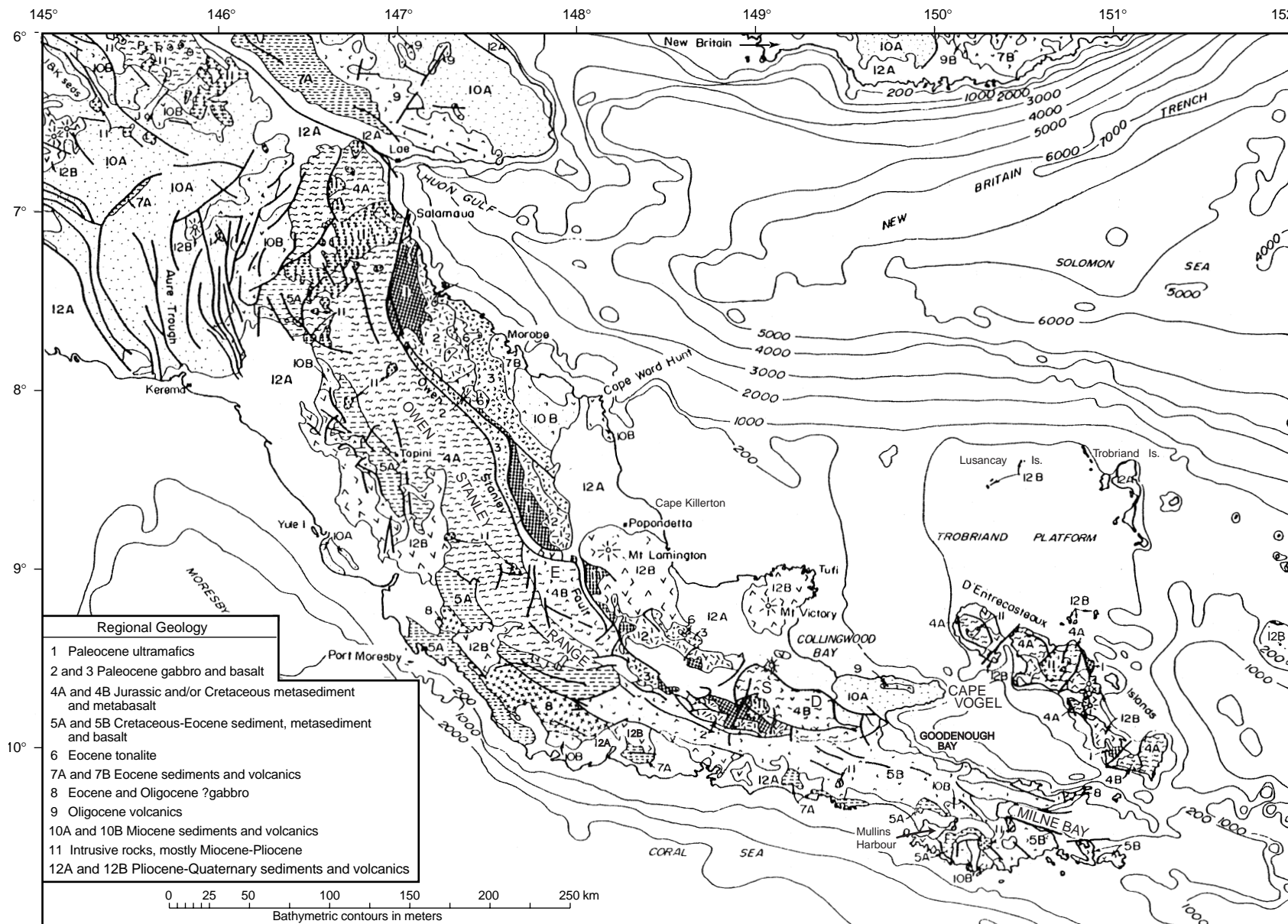


Figure F3. Ages, locations, and associations of Miocene (A) and Pliocene–Pleistocene (B) volcanism in eastern Papua, modified after Smith and Milsom (1984).

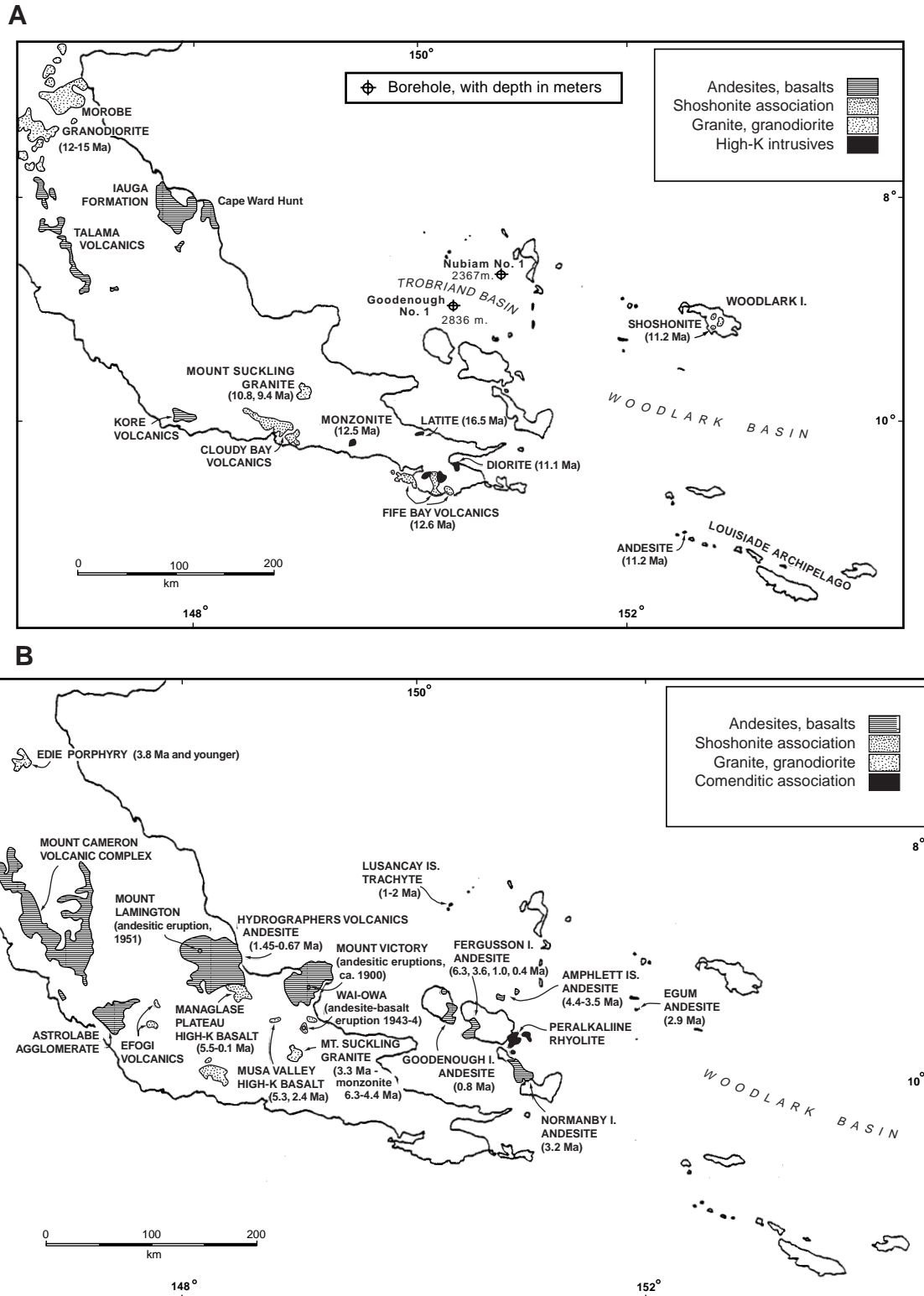


Figure F4. A. Depth to basement in the western part of the Trobriand forearc basin (Cape Vogel Basin), modified after Pinchin and Bembrick (1985). (Continued on next page.)

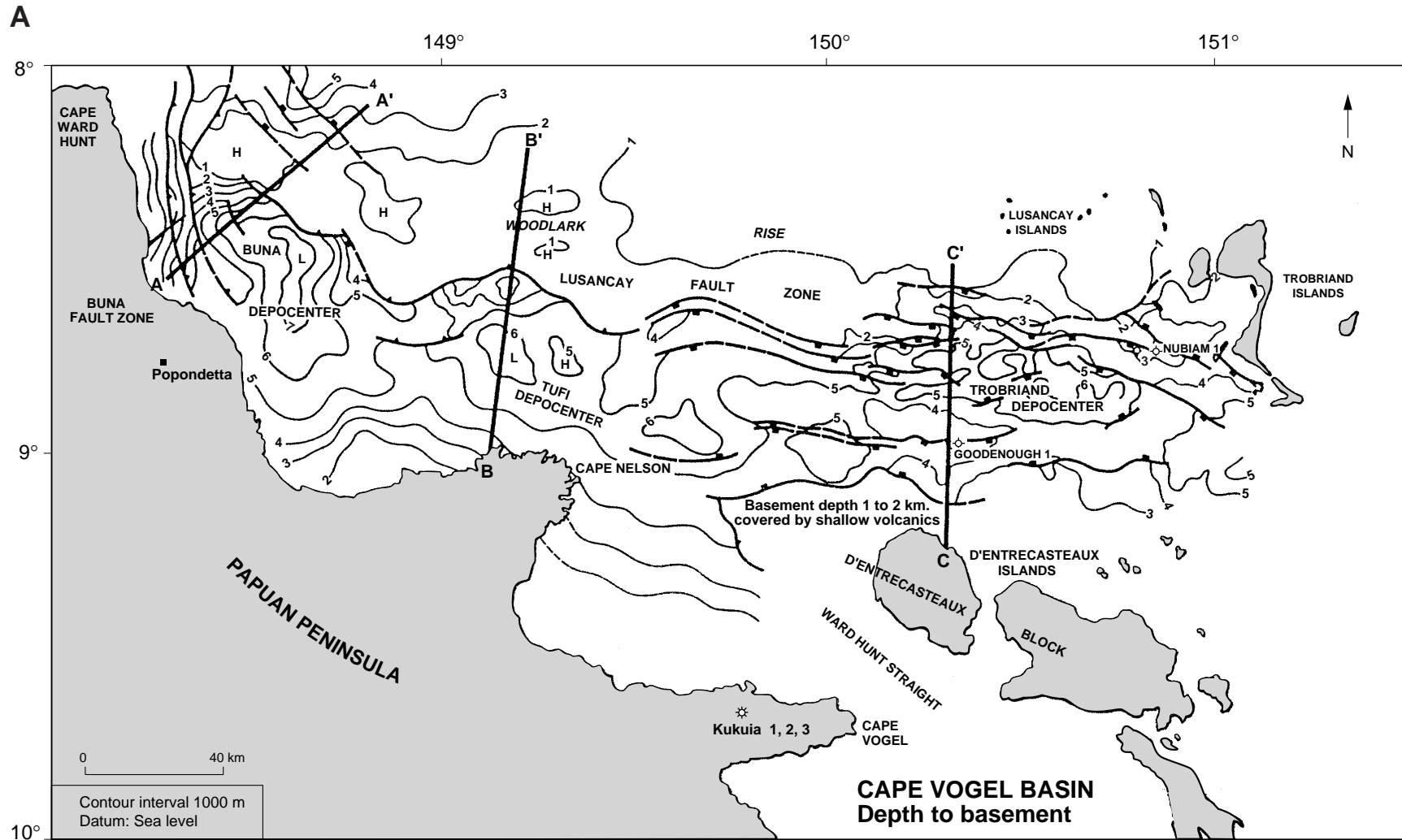


Figure F4 (continued). B. Line drawing cross sections of the western part of the Trobriand forearc basin (Cape Vogel Basin), modified after Pinchin and Bembrick (1985).

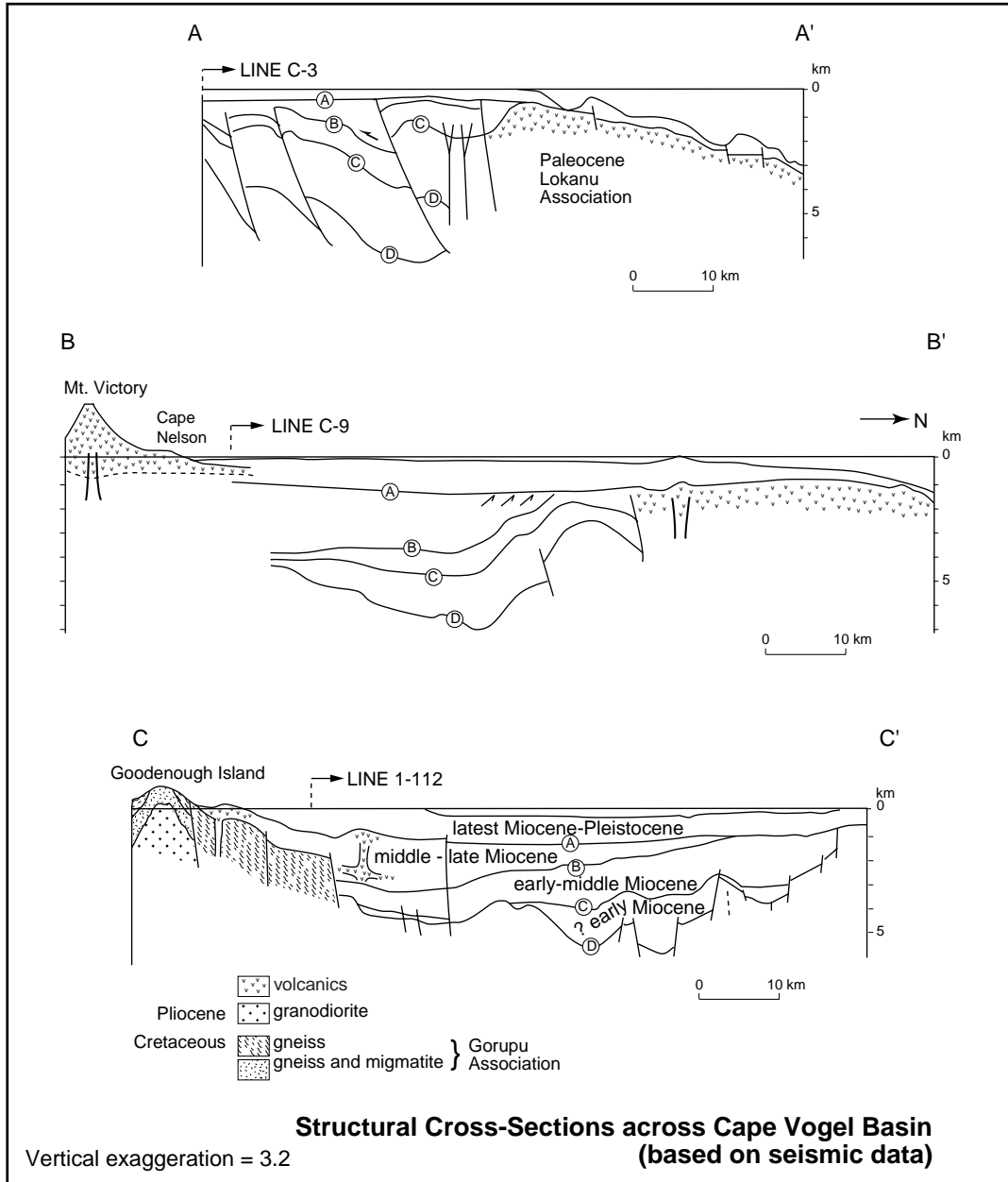


Figure F5. Well correlation diagram, Goodenough-1 to Nubiam-1, showing the biostratigraphy, lithologies and regional unconformities. Modified after Francis et al., 1987.

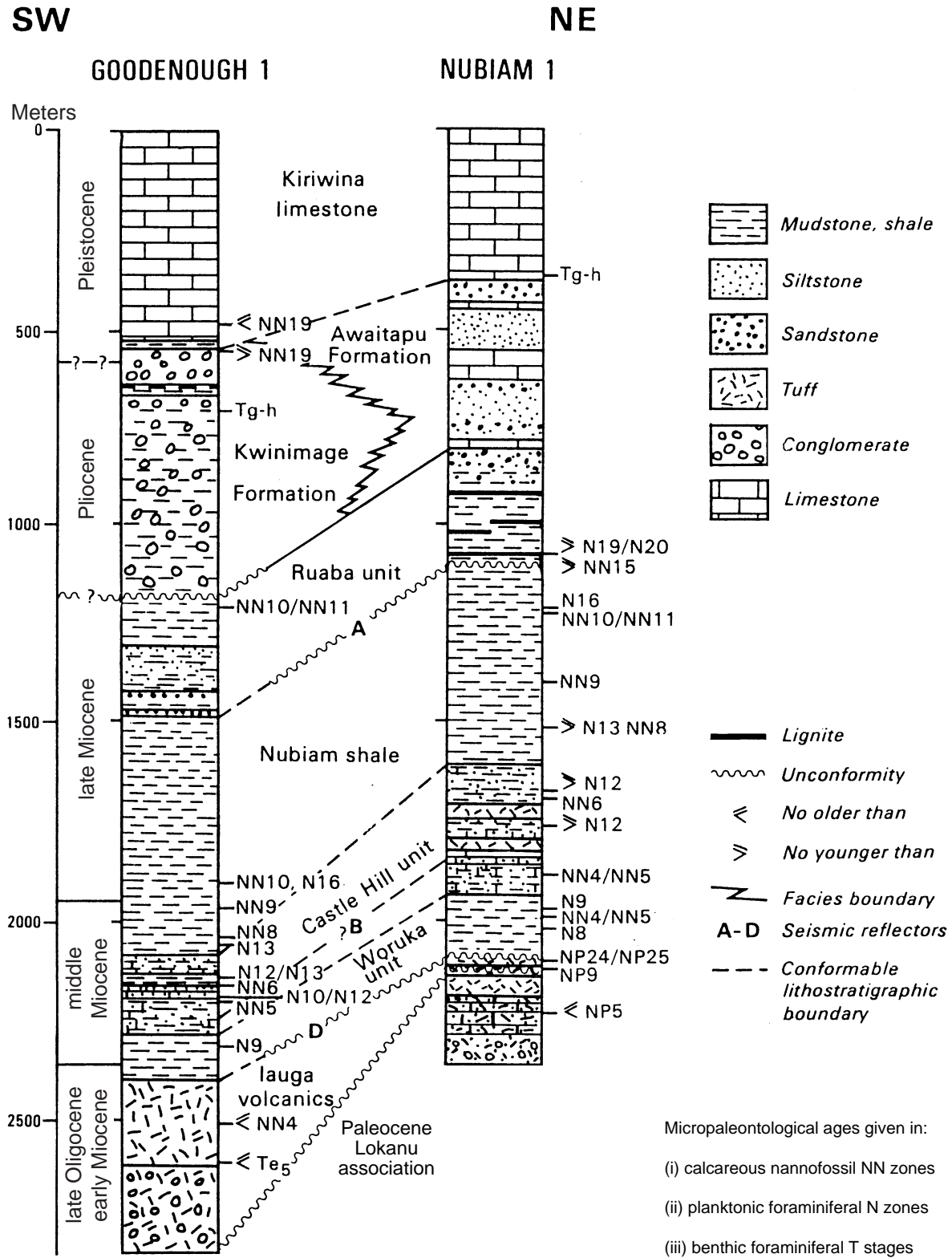


Figure F6. Parallel seismic reflection profiles, located in Figure F7A, p. 20, with highlighted unconformity reflectors (A–D, lower profile) that have been tied to wells and regionally correlated throughout the Trobriand Basin. Line 1-112 modified after Davies and Warren (1988). Line 1-114 modified after Stewart et al. (1986).

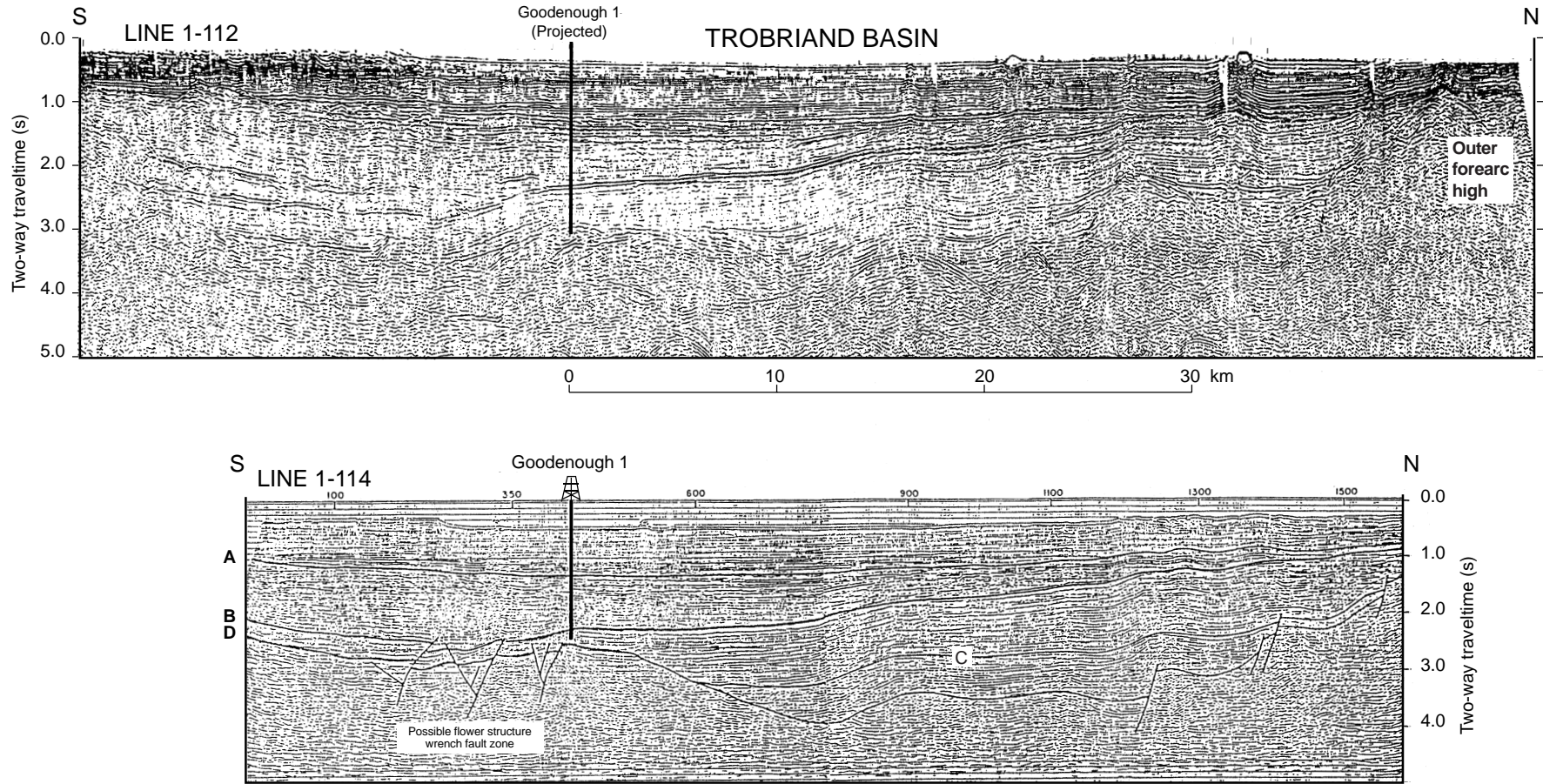


Figure F7. A. Location of wells and seismic reflection lines in the Trobriand Basin (Block PNG/15P), modified after Tjin (1976). Lines 1–112 and 1–114, shown in Figure F6, p. 19, are highlighted. **B.** Sparker profile BMR05-163 (location on Fig. F7A below) in the northwest Woodlark Basin (from Davies et al., 1984) shows slope-parallel reflectors above a northward-migrating progradational facies that lies just below the sequence boundary. This unconformity can be jump-correlated across the Trobriand reef front at 151°10'E to unconformity A (Figs. F4A, p. 16, F4B, p. 17, F5, p. 18, F6, p. 19). The forearc basin sediments below are seen to lap onto the basement of the outer forearc high.

